Simulation of Acoustic Scattering from Undersea Targets in Shallow Water

David S. Burnett & Mario Zampolli
NATO Undersea Research Center
Viale S. Bartolomeo 400
19138 La Spezia
Italy

burnett@saclantc.nato.int / zampolli@saclantc.nato.int

ABSTRACT

The Centre has developed a 3-D finite-element structural acoustics code for modeling the scattering of minehunting sonar from undersea mines. 3-D continuum mechanics is used throughout, including even for thin structural components such as plates and shells. The code is therefore fully 3-D in both physics and geometry. The paper describes an unusual approach to code development, briefly explains the underlying physics and mathematics, and presents several scattering and propagation models, including mine/decoy discrimination and scattering in shallow water.

1.0 INTRODUCTION

The Centre initiated a research effort five years ago to develop a high-fidelity 3-D finite-element structural acoustics code for modeling the scattering of minehunting sonar from undersea mines located in or near the seabed in shallow water. To achieve high fidelity, thin structural components, such as plates and shells, are modeled with 3-D physics rather than plate or shell theories, the latter employing 2-D physics inside a 3-D geometry. The code is therefore fully 3-D in both physics and geometry. The rationale for this approach is as follows. Undersea mines are typically enclosed thin shells with interior reinforcements such as rib-stiffeners or partitions, exterior attachments, and sometimes abrupt edges or corners. These irregularities are geometric discontinuities, in the vicinity of which the deformation state during vibration is strongly 3-D, consisting of localized (evanescent) 3-D elastic waves. The latter determine the amplitude and phase of the elastic waves that propagate throughout the shell, which in turn determine the amplitude and phase of the acoustic waves "launched" into the exterior water. In short, the scattered sonar signal may depend strongly on the localized 3-D elastic waves in the shell. The first version of a steady-state (time-harmonic) code, named FESTA, for Finite Element Structural Acoustics, was released in 2003.

2.0 CODE DEVELOPMENT APPROACH

The Centre is using the commercial software package ProPHLEX [1] developed by the R&D Division of Altair Engineering (formerly COMCO). This package is a suite of software tools for *developing* customized finite-element (FE) codes. It contains a library of several thousand routines [O(10^6) lines] that perform all the detailed tasks of an FE analysis. To develop an application code, the researcher derives the Galerkin residual equations from the governing partial differential equations (PDEs) and then links self-written code [O(10^3) lines] with the vendor-written library, which creates an application code with a commercial-quality GUI, e.g., FESTA. A central feature of ProPHLEX is its *hp*-adaptivity – an automated procedure for achieving near-optimal FE meshes, based on the use of high-order "hierarchic" basis functions and element-by-element error estimators.

Paper presented at the RTO SET Symposium on "Capabilities of Acoustics in Air-Ground and Maritime Reconnaissance, Target Classification and Identification", held in Lerici, Italy, 26-28 April 2004, and published in RTO-MP-SET-079.

ProPHLEX is applicable to any system or process that can be mathematically formulated as a system of coupled 2nd-order PDEs, which is expressed here on the left in tensor notation and, equivalently, on the right in vector-matrix notation:

$$\left(a_{\alpha l \beta m} q_{\beta,m}\right)_{,l} + b_{\alpha \beta m} q_{\beta,m} + c_{\alpha \beta} q_{\beta} = -f_{\alpha} \qquad \text{or} \qquad \nabla \bullet \left(\boldsymbol{a} \nabla \boldsymbol{q}\right) + \boldsymbol{b} \nabla \boldsymbol{q} + \boldsymbol{c}\boldsymbol{q} = -\boldsymbol{f} \qquad (1)$$

Referring to the tensor formulation, which is the more natural to work with in continuum mechanics, a comma subscript means partial differentiation with respect to the independent variables, i.e., $(\,)_{,i} = \partial(\,)/\partial x_i$, where, for physically oriented systems, x_i are usually the spatial coordinates. The components of the vector q_β may be any meaningful quantities, but q_β need not be sensible as a vector. For example, the components can include displacements in an elastic solid and pressures in an acoustic fluid. The coefficients $a_{\alpha l \beta m}$, $b_{\alpha \beta m}$ and $c_{\alpha \beta}$ are tensors of 4th, 3rd and 2nd-orders, respectively. They may be a function of q_β (for nonlinear processes), a function of the independent variables x_i (for spatial inhomogeneities) and a function of time (for transient processes). All variables must be real-valued; hence, any PDEs with complex variables must be decomplexified. Equation (1) can describe a very broad range of phenomena, including the coupling of different types of phenomena.

ProPHLEX uses eq. (1) in each and every finite element in the computational domain. Therefore, to develop a structural acoustics code, the analyst must cast the governing PDEs for both the vibrating solid and acoustic fluid into a single system of PDEs in the form of eq. (1). This, in effect, treats the entire fluid-structure domain as a single continuum, which is modeled using only one type of finite element: a fluid-solid element.

3.0 A UNIFIED CONTINUUM MECHANICS DERIVATION OF A FLUID-SOLID ELEMENT

Both the solid and the fluid are elastic media, experiencing small, steady-state vibrations about a quiescent state. The solid may be viscoelastic, anisotropic and inhomogeneous. The fluid is inviscid but may include volume dissipation, and is isotropic and inhomogeneous. Under these conditions, *the continuum mechanics for the fluid are a special case of those for the solid*. Hence, to derive the acoustic wave equation for the fluid, one may begin with the governing PDEs for wave propagation in an elastic solid and apply the appropriate limiting conditions.

Thus, beginning with the solid, a conventional derivation yields the following steady-state wave equation for a viscoelastic solid, again showing tensor notation on the left and vector-matrix notation on the right,

$$\left(\hat{c}_{\alpha l \beta m} \hat{u}_{\beta,m}\right)_{,l} + \omega^2 \rho^s \hat{u}_{\alpha} = -\hat{f}^s_{\alpha} \qquad \text{or} \qquad \nabla \bullet \left(\hat{\boldsymbol{c}} \nabla \hat{\boldsymbol{u}}\right) + \omega^2 \rho^s \hat{\boldsymbol{u}} = -\hat{\boldsymbol{f}}^s \qquad (2)$$

where the circumflex, ^, denotes a complex-valued quantity. The coefficient $\hat{c}_{\alpha l \beta m}$ contains a fully anisotropic set of elastic moduli, $\hat{u}_\alpha$ is particle displacement, ρ^s is solid density, $\hat{f}^s_\alpha$ is a solid body force and ω is circular frequency.

For the fluid, one begins with the various PDEs used to derive eq. (2) and applies appropriate limiting conditions for an isotropic fluid, being careful to separate volumetric and shear deformations. This approach yields the steady-state acoustic wave equation, i.e., Helmholtz equation, shown here in both tensor and vector-matrix notations,

$$\left(\frac{1}{\omega^2\rho^f}\hat{p}_{,m}\right)_{,m}+\frac{1}{\hat{B}}\hat{p}=0 \qquad \text{or} \qquad \nabla\bullet\left(\frac{1}{\omega^2\rho^f}\nabla\hat{p}\right)+\frac{1}{\hat{B}}\hat{p}=0 \tag{3}$$

where $\hat{p}$ is acoustic pressure, ρ^f is fluid density and $\hat{B}$ is bulk modulus.

Equation (3) is appropriate for inhomogeneous media, i.e., where ρ^f or $\hat{B}$ may vary with position. This includes multiple homogeneous fluids, where ρ^f and $\hat{B}$ are piecewise constant but with discontinuities at fluid-fluid interfaces. At such an interface it is necessary that particle displacement normal to the interface be continuous (conservation of mass). Since the operand of the divergence operator is particle displacement (which follows from "Euler's equation" for balance of linear momentum), application of the divergence theorem in the FE Galerkin procedure will produce a surface integral enabling one to specify continuity of normal displacement at the interface. [A similar argument can be made for the inhomogeneous viscoelastic wave equation in eq. (2), where the divergence operand is stress, enabling one to specify continuity of normal stress across interfaces of dissimilar materials.]

The wave equations in both media, eqs. (2) and (3), are decomplexified and then combined into a single tensor wave equation in the form of eq. (1), where

$$q_\beta=\begin{Bmatrix} u_x^s \\ u_y^s \\ u_z^s \\ u_x^f \\ u_y^f \\ u_z^f \\ p^s \\ p^f \end{Bmatrix}\begin{matrix}\uparrow \\ \text{displacement} \\ \text{in solid} \\ \downarrow \\ \uparrow \\ \text{pressure} \\ \text{in fluid} \\ \downarrow\end{matrix}, \qquad a_{\alpha l\beta m}=\begin{array}{c|c|c|c|c|c|c|c|c} \beta=1 & 2 & 3 & 4 & 5 & 6 & 7 & 8 & \\ \hline c^R_{\alpha l\beta m} & & & -c^I_{\alpha l(\beta-3)m} & & & 0 & & \alpha=1 \\ & & & & & & & & 2 \\ & & & & & & & & 3 \\ \hline c^I_{(\alpha-3)l\beta m} & & & c^R_{(\alpha-3)l(\beta-3)m} & & & 0 & & 4 \\ & & & & & & & & 5 \\ & & & & & & & & 6 \\ \hline 0 & & & 0 & & & \frac{1}{\omega^2\rho^f}\delta_{\alpha\beta}\delta_{lm} & & 7 \\ & & & & & & & & 8 \end{array}, \tag{4}$$

$$c_{\alpha\beta}=\begin{array}{c|c|c|c|c|c|c|c|c} \beta=1 & 2 & 3 & 4 & 5 & 6 & 7 & 8 & \\ \hline \omega^2\rho^s\delta_{\alpha\beta} & & & 0 & & & 0 & & \alpha=1 \\ & & & & & & & & 2 \\ & & & & & & & & 3 \\ \hline 0 & & & \omega^2\rho^s\delta_{\alpha\beta} & & & 0 & & 4 \\ & & & & & & & & 5 \\ & & & & & & & & 6 \\ \hline 0 & & & 0 & & & K_{\alpha\beta} & & 7 \\ & & & & & & & & 8 \end{array}$$

and $b_{\alpha\beta m} = 0$. The superscripts R and I indicate real and imaginary parts, respectively. The first 6 rows of f_α contain the real and imaginary parts of $\hat{f}^s_\alpha$; the last 2 rows are zero. Equation (4)

shows the α,β-"plane" of $a_{\alpha l \beta m}$; each of the 64 positions is a 3×3 tensor in l,m, where l,m = 1,2,3 for the 3 spatial coordinates. The tensors $c^R_{\alpha l \beta m}$ and $c^I_{\alpha l \beta m}$ are the real and imaginary parts, respectively, of the complex elastic moduli and $K_{\alpha\beta}$ is the decomplexified fluid compressibility, which is derived from the reciprocal of the complex bulk modulus.

Equations (1) and (4) are a system of eight coupled 2nd-order PDEs describing wave propagation in both solids and fluids. Using the FE Galerkin procedure, this system of PDEs is transformed to a matrix equation for a 3-D *hp*-adaptive solid-fluid finite element (brick, wedge and tet), which is the only element needed in FESTA.

4.0 VERIFICATION PROBLEMS

4.1 Scattering from thin-walled elastic spherical shell in unbounded fluid

One of the first and most basic test problems used for code verification in structural acoustics is scattering of a plane wave from an elastic, thin-walled spherical shell in an unbounded fluid, since an analytical ("exact") solution can be derived. For this example the shell is steel and the fluid is water. The shell's wall thickness is 5% of its outer radius. A spherical body of water surrounds the shell, with a radius twice that of the shell. A 1st-order Bayliss-Turkel radiation condition is applied on the outer boundary of the water to absorb the outward propagating scattered field, thus simulating an unbounded fluid. [The B-T condition is easy to program and thus was useful for the first version of FESTA; it is currently being replaced by infinite elements, which have much greater computational efficiency.]

The analysis was performed at ka = 40, where $k = \omega/c$ is the wavenumber and a is the radius of the sphere. The problem is axisymmetric so only one quadrant of the shell and water was modeled. The mesh on one face of the quadrant is shown in Fig. 1(a). It used cubic elements in the fluid, with 4 degrees of freedom (DOF)/wavelength, and quartic elements in the shell, with about 5 DOF/wavelength. Using the decomposition $\hat{p}^{total} = \hat{p}^{inc} + \hat{p}^{scat}$ (which is simply a definition of $\hat{p}^{scat}$), FESTA computed $\hat{p}^{scat}$ directly, then in postprocessing added $\hat{p}^{inc}$ to $\hat{p}^{scat}$ to obtain $\hat{p}^{total}$. Figure 1(b) shows contours of pressure magnitude, $|\hat{p}^{total}|$, and Fig. 2 plots the real and imaginary parts of $\hat{p}^{total}$ along a path close to the sphere and parallel to a meridian from 0° (incident direction) to 180°.

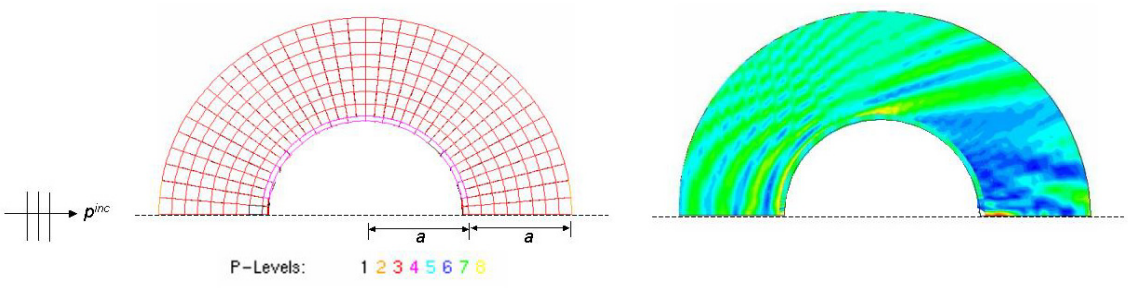

Figure 1: (a) FE mesh for immersed spherical shell, (b) Contours of $|\hat{p}^{total}|$.

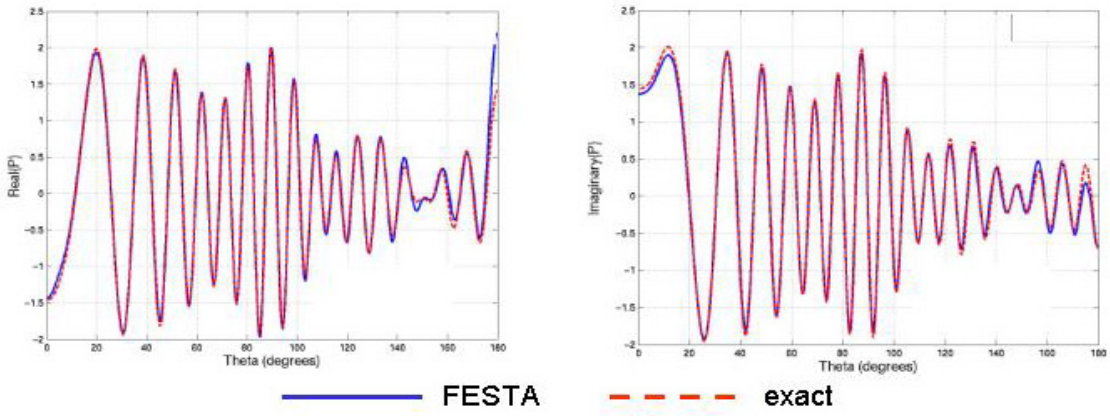

Figure 2: (a) Real part of $\hat{p}^{total}$ along meridianol path, (b) imaginary part along same path.

4.2 Scattering from a rough interface between two fluids

To test just the acoustics, a FESTA model of acoustic propagation and scattering from a fluid interface is compared with a solution from an independent computer code, COUPLE [2], that is based on a non-FE technique, viz., coupled normal modes. Figure 3 describes the physical problem: a 30 Hz monopole source is located 100m above a water/sediment interface that has square-cut grooves in a circular pattern. The problem is axisymmetric. Since FESTA is 3-D, a wedge-shaped slice, shown in the figure, is used for the FE model, with symmetry boundary conditions on the wedge faces. The green shading indicates the vertical-radial plane (not to scale) in which the computed field is displayed. Figure 4 shows the FE mesh in the green-shaded plane in Fig. 3; the full 3-D mesh is created by rotating this mesh, about the axis of symmetry, through the wedge-shaped slice. Figure 5 displays in the green-shaded plane the contours of transmission loss (TL) computed by FESTA. Figure 6 compares the TL values computed by FESTA and COUPLE, along the dashed line in Fig. 5.

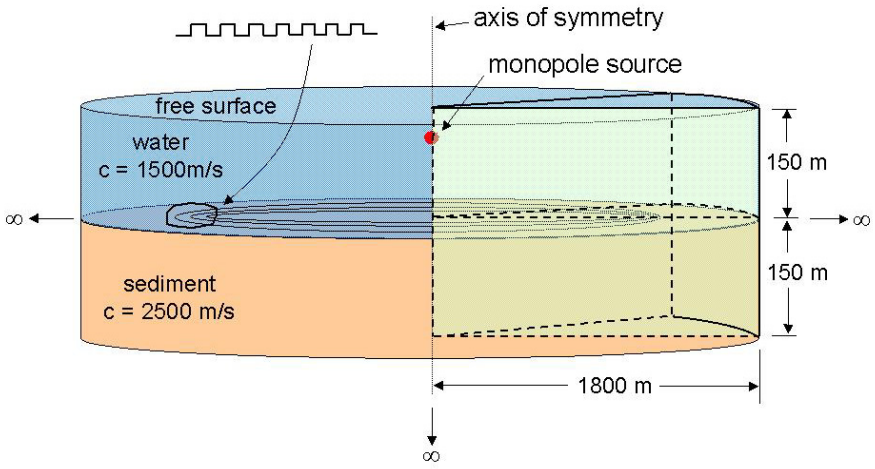

Figure 3: Monopole source above water/sediment interface with square-cut circular grooves.

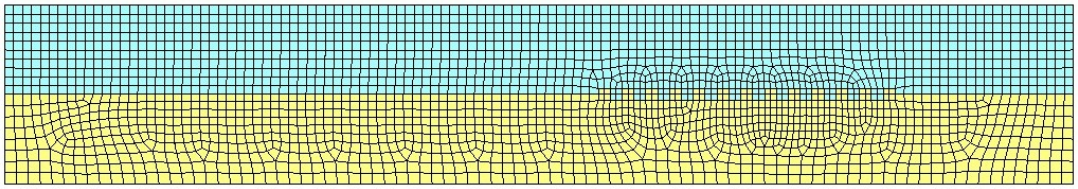

Figure 4: FE mesh on face of wedge in Fig. 3.

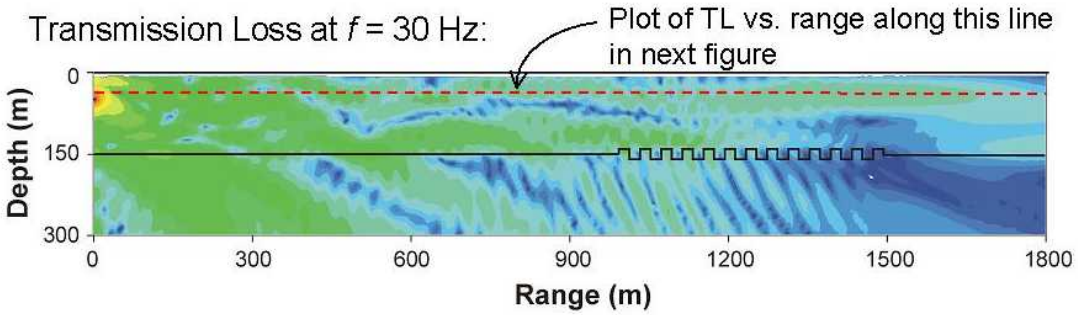

Figure 5: Contours of TL computed by FESTA.

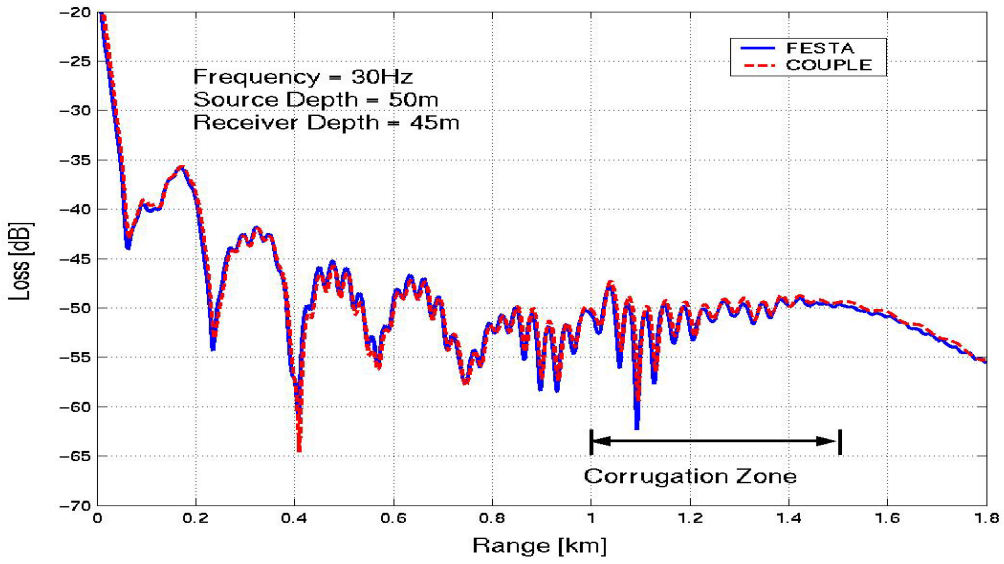

Figure 6: Comparison of TL computed by FESTA and COUPLE.

5.0 REALISTIC APPLICATION PROBLEMS

5.1 Scattering from Manta mine and Manta decoy in unbounded water

This problem illustrates the ability of FESTA to distinguish a real mine from an identically shaped decoy. Figure 7 shows views of an actual Manta mine. Figure 8(a) is a FE model of the mine, including the fiberglass casing and internal materials such as the explosive, priming device and water. Part (b) is a FE model of a possible decoy, in which the fiberglass casing is identical but most of the internal materials have been replaced by concrete. The mine and decoy are immersed in unbounded water and each is insonified by a plane wave, incident at 7.5^{o} above horizontal. Figures 9(a) and 9(b) are polar plots in a vertical plane, at 1 kHz (ka = 2) and 5 kHz (ka = 10), respectively, of the total-field intensity levels, $20Log|\hat{p}^{total}|$. The levels are evaluated on a circular path close to and surrounding the mine and decoy. At the lower frequency, ka = 2, there is a larger *difference* between the Manta and decoy responses than at ka = 10, which provides a mechanism for distinguishing the real mine from the decoy. This illustrates the well-known principle that at low frequencies, where wavelengths are comparable to the dimensions of the target, the resonances of the internal structure cause a significant change in the scattered acoustic field, but at higher frequencies the internal structure has less of an effect. Indeed, at much higher frequencies, e.g., in the band of acoustic imaging, it is difficult, if not impossible, to distinguish a decoy from a real mine.

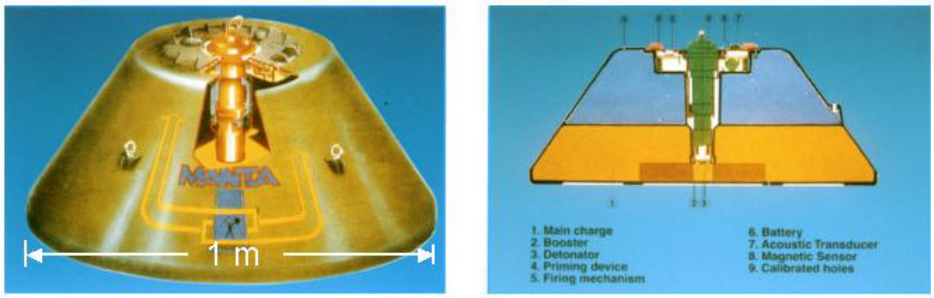

Figure 7: Cutaway and cross-sectional views of Manta mine.

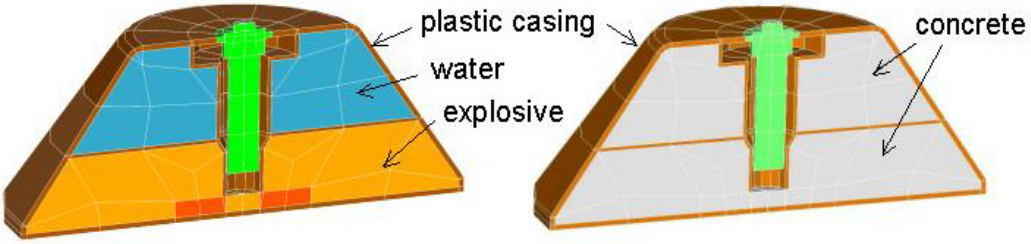

Figure 8: (a) FE model of Manta mine, (b) FE model of Manta decoy.

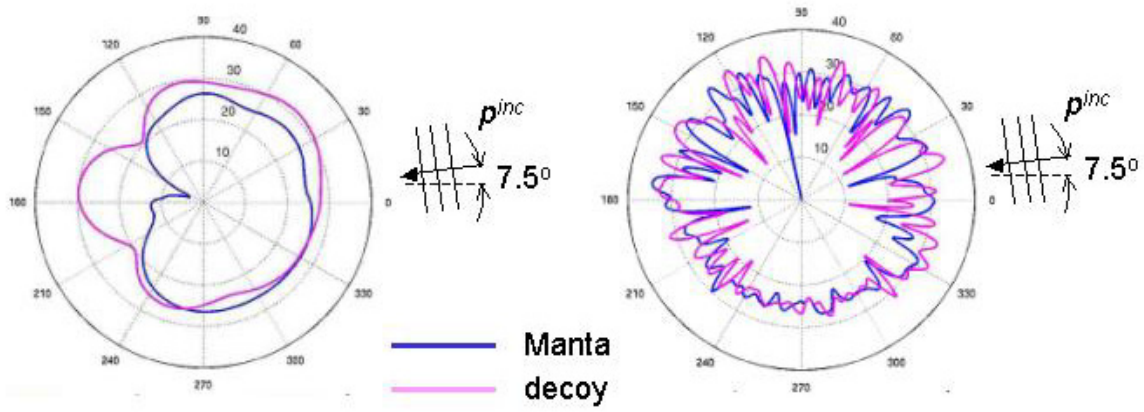

Figure 9: (a) 20 Log | $\hat{p}^{total}$ | at 1 kHz (ka = 2), (b) 20 Log | $\hat{p}^{total}$ | at 10 kHz (ka = 20).

5.2 Scattering from Manta mine on seabed in shallow water

Using the above MANTA FE mesh, the mine is now placed on a sedimentary seabed in 100m-deep water (Fig. 10). [A depth of 10 - 200m is "shallow" in NATO undersea operations.] The ocean surface and water/sediment interface are flat. The sediment is modeled as a heavy, dissipative fluid. A 1 kHz monopole source is located at a range of 500m from the mine and a depth of 30m. Although FESTA can model scattering in complex waveguides (as will be shown by one of the verification problems in the oral presentation), this computational domain is too large in terms of wavelengths, λ, for available computer resources. Since λ = 1.5m, the source/mine separation is 333λ and the depth is 67λ. A high-accuracy 3-D scattering model would require several tens of millions of DOF. Therefore a more efficient *hybrid* approach is employed. FESTA is used only to compute the *local* target scattering, i.e., the elastic waves inside the target and the scattered field in the *vicinity* of the mine (within a few wavelengths from the mine). A non-FE propagation code computes the *global* propagation of the incident and scattered fields throughout the waveguide. The propagation code used in this problem is OASES [3], which is based on wavenumber integration. This approach requires three separate analyses, performed in a specific sequence, with the output from one step becoming the input to the next:

- 1st step: OASES computes p^{inc} throughout the waveguide, which, by definition, is the acoustic field in the absence of the target.
- 2nd step: FESTA computes the local scattered field, p^{scat}_{local} , modeling the target inside a small sphere containing the fluid(s) immediately surrounding the target. The fields p^{inc} and p^{scat}_{local} are input and output, respectively, on the surface of the sphere. The Bayliss-Turkel radiation condition is applied to p^{scat}_{local} on the sphere, which, in effect, models an infinite domain with no other scatterers present -- an acceptable approximation if scatterers are in fact present, e.g., the sea surface, but are separated from the target by several target diameters.
- 3rd step: OASES, using p^{scat}_{local} as input data, computes the scattered field throughout the waveguide, p^{scat}_{global} , which is the desired final solution from the 3-step process, shown below in Fig. 11.

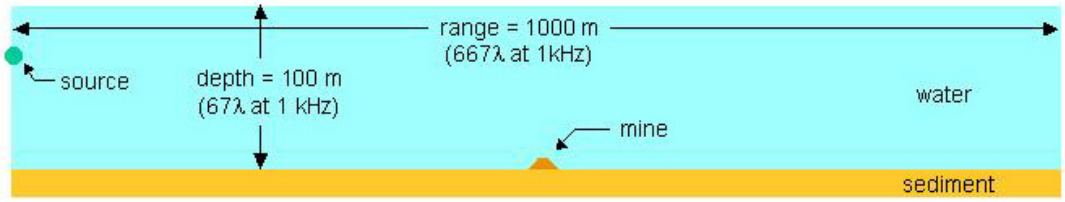

Figure 10: Manta mine on seabed in shallow water, insonified by 1 kHz monopole source.

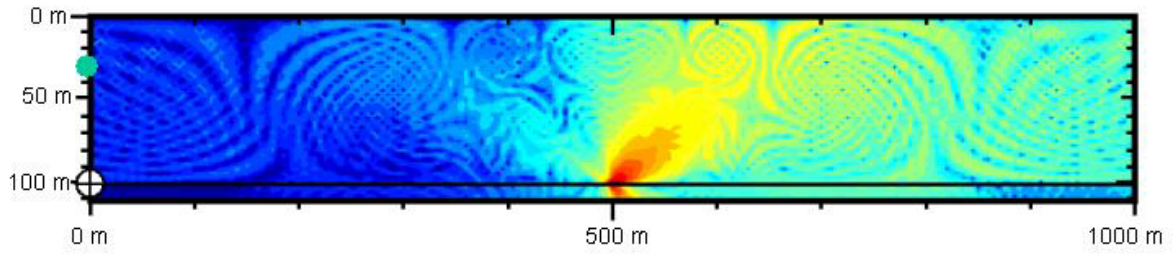

Figure 11: Contours of scattered-field intensity level, 20 Log | $\hat{p}^{scat}$ |.

5.3 Scattering from cylinder partially buried in seabed in shallow water

A second hybrid approach has also been developed. It involves fewer steps and employs FESTA in a manner that is independent of the environment, permitting the FESTA analysis to be reused for different environments. In this approach, an admittance matrix is computed for the target *in vacuo* (no surrounding fluid). Defining a grid of points covering the outer surface of the target, a time-harmonic normal "point" force (actually, distributed over a small area) is applied successively to each grid point, a process that may be thought of as a movable virtual shaker. For each force, normal displacements are computed at all the grid points. For n grid points, this creates an $n \times n$ matrix, which is the admittance matrix. It characterizes the interaction of the target with any external environment.

The n analyses employ the same assembled and reduced FE system (stiffness and mass) matrix; only the load vectors vary. Hence each analysis involves only a reduction of each load vector followed by a back-substitution, both of which are inexpensive (n^2) operations. The entire matrix is analyzed in an automated loop over all the load vectors. The admittance matrix may then be input to OASES which computes both p^{inc} and p^{scat} in a single analysis. The principal advantage of this method is the one-time-only analysis of the target, which can then be used in any environment (buried, partially buried, floating) under any insonification. A probable limitation is the very large data set associated with the admittance matrix: the size of the matrix increases exponentially with frequency, which will place a practical upper bound (not yet known) on frequency.

To illustrate this approach, consider a waveguide similar to the one above, with a sedimentary seabed and 100m-deep water, though the range is now 2000m and the source is a 2.5 kHz monopole at a depth of 50m (Fig. 12). The target, at a range of 1000m from the source, is a half-buried steel cylinder with hemispherical endcaps that is tilted 45° upwards and 45° to the side. The cylinder length is 60cm, the endcap outer radius is 9.08cm and the wall thickness is 0.6cm. FESTA first computed the in-vacuo admittance matrix for the cylinder. The matrix was then input to OASES, which computed the scattered field (Figs. 13 and 14).

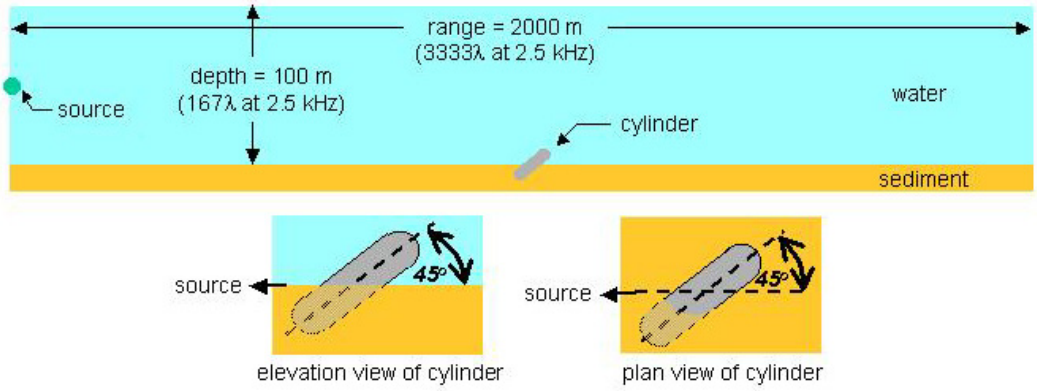

Figure 12: Half-buried cylinder on seabed in shallow water, insonified by 2.5 kHz monopole source.

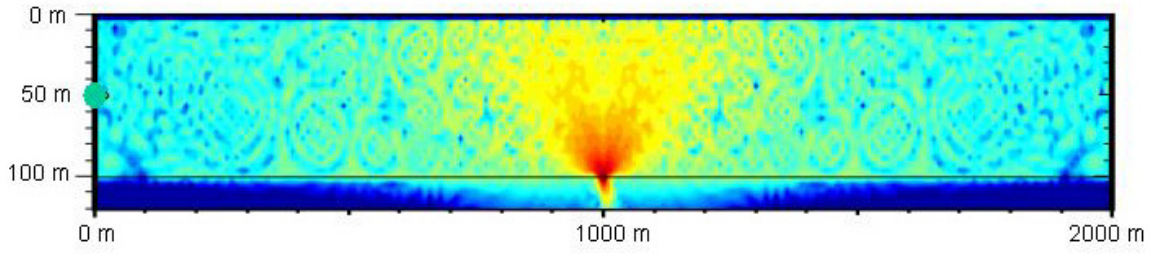

Figure 13: Contours of scattered-field intensity level, $20\,\mathrm{Log}\,|\,\hat{p}^{\,scat}\,|$, in vertical plane.

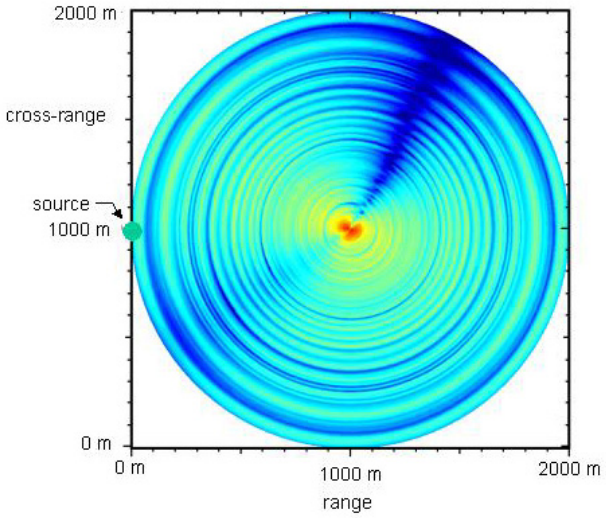

Figure 14: Contours of scattered-field intensity level, $20\,\mathrm{Log}\,|\,\hat{p}^{\,scat}\,|$, in horizontal plane 10m above sediment.

6.0 ACKNOWLEDGEMENTS

Dr. Finn Jensen, the program manager, has provided valuable support throughout the project, both technical and administrative. Dr. John Blottman, a visiting scientist from NUWC in Newport, R.I., made several contributions to FESTA, including assistance with the hybrid approach. Dr. Henrik Schmidt at M.I.T. has made a substantial contribution to the hybrid approach through his continuing collaboration involving his OASES code.

7.0 REFERENCES

[1] T.J. Liszka, W.W. Tworzydlo, J.M. Bass, S.K. Sharma, T.A. Westerman, B.B. Yavari, "ProPHLEX -- An *hp*-adaptive finite element kernel for solving coupled systems of partial differential equations in computational mechanics", Comput. Methods Appl. Mech. Engrg., Vol. 150, 1997, pp. 251-271.

[2] R.B. Evans, "A coupled mode solution for acoustic propagation in a waveguide with step-wise depth variations of a penetrable bottom", J. Acoust. Soc. Amer., Vol. 74, 1983, pp. 188-195.

[3] H. Schmidt, "OASES, Version 3.1, User Guide and Reference Manual", Dept. of Ocean Engrg., M.I.T., 2003. (Available at http://acoustics.mit.edu/faculty/henrik/oases.html.)